$^{40}Ar/^{39}Ar$ geochronology from South Australian samples in the AuScope National Argon Map project 1: Gawler Craton

Anthony Reid[1], Marnie Forster[2], Davood Vasegh[2],

[1]Geological Survey of South Australia, Department for Energy and Mining
[2]Argon Laboratory, Research School of Earth Sciences, Australian National University

July 2022

Report Book 2022/00007

Department for Energy and Mining
Level 4, 11 Waymouth Street, Adelaide
GPO Box 320, Adelaide SA 5001
Phone +61 8 8463 3000
Email dem.minerals@sa.gov.au
dem.petroleum@sa.gov.au
www.energymining.sa.gov.au

South Australian Resources Information Gateway (SARIG)
SARIG provides up-to-date views of mineral, petroleum and geothermal tenements and other geoscientific data. You can search, view and download information relating to minerals and mining in South Australia including tenement details, mines and mineral deposits, geological and geophysical data, publications and reports (including company reports).
map.sarig.sa.gov.au

Disclaimer

The contents of this report are for general information only and are not intended as professional advice, and the Department for Energy and Mining (and the Government of South Australia) make no representation, express or implied, as to the accuracy, reliability or completeness of the information contained in this report or as to the suitability of the information for any particular purpose. Use of or reliance upon the information contained in this report is at the sole risk of the user in all things and the Department for Energy and Mining (and the Government of South Australia) disclaim any responsibility for that use or reliance and any liability to the user.

Acknowledgement of Country

The Department for Energy and Mining acknowledges Aboriginal people as the First Nations Peoples of South Australia. We recognise and respect the cultural connections as the traditional owners and occupants of the land and waters of South Australia, and that they continue to make a unique and irreplaceable contribution to the state.

Preferred way to cite this publication

Reid A, Forster M and Vasegh D 2022. *^{40}Ar/^{39}Ar geochronology from South Australian samples in the AuScope National Argon Map project 1: Gawler Craton*, Report Book 2022/00007. Department for Energy and Mining, South Australia, Adelaide.

CONTENTS

TABLES

FIGURES

$^{40}Ar/^{39}Ar$ geochronology from South Australian samples in the AuScope National Argon Map project 1: Gawler Craton

Anthony Reid, Marnie Forster and Davood Vasegh

ABSTRACT

The National Argon Map is an AuScope-funded pilot project (2020–2021). The project aimed to compile a national-scale map of and to analyse new samples to fill the gaps in national coverage in $^{40}Ar/^{39}Ar$ geochronology. This report provides the results from samples in the eastern Gawler Craton, in the vicinity of the Olympic Dam deposit, and from the region in and around the Cairn Hill Fe-Cu deposit. Hydrothermal muscovite from drill hole ASD 1 yields a discordant age spectrum with upper limit of c. 952.8 Ma and lower limit of c. 496.6 Ma, suggesting overprinting during the Delamerian Orogeny. K-feldspar from drill hole Blanche 1, located around 6 km to the southwest of the Olympic Dam ore deposit yields a complex spectrum that includes four age populations, 1500.6 ± 9.2 Ma, 1406.2 ± 5.7 Ma, 1153.7 ± 4.2 Ma, and c. 682.8 Ma, suggesting multi-phase hydrothermal processes have affected this granite. Analysis of hornblende from a narrow vein of hornblende-magnetite alteration within the Cairn Hill deposit yields a plateau age of 1412.5 ± 3.7 Ma, which may record the timing of formation of this hornblende. Conversely, K-feldspar from the foliated granite that hosts the hornblende-magnetite vein yields a step-wise age progression from an upper limit of 1278.9 ± 6.7 Ma and a lower limit of 995.0 ± 6.6 Ma, suggesting Musgravian-aged thermal and or microstructural events have affected the K-feldspar in the sample. Biotite and K-feldspar was also analysed from a sample of foliated and partly altered granite from drill hole KDD005, to the west of Cairn Hill. The biotite has a disturbed age spectra with an upper limit of 1506.5 ± 8.6 Ma and an intermediate limit of 1430.7 ± 4.1 Ma, suggesting overprinting during the regional c. 1465 – 1410 Ma thermal event documented previously across the northern Gawler Craton. The co-existing K-feldspar in contrast records an upper age limit of 1355 ± 5.6 Ma and a lower limit of 1206.2 ± 7.7 Ma, suggesting overprinting during a Musgravian-aged thermal or microstructural event, thereby further extending the spatial distribution of rocks that have evidence for Musgravian-age processes that have affected them across the Gawler Craton. Further work is required to produce a more complete interpretation of the data presented here, including analysis of diffusion parameters derived during the step-heating experiments.

INTRODUCTION

The National Argon Map (NAM) project is an AuScope Pilot Project led by Dr Marnie Forster at the Australian National University and overseen by an independent advisory panel led by Dr Geoff Fraser of Geoscience Australia. It is a collaboration with the National Argon Network, involving the Argon laboratories at the Australian National University, Curtin University, the University of Queensland and Melbourne University.

The data compilation that the NAM undertook is presented in an online database and map accessible via https://www.google.com/maps/d/viewer?usp=sharing&mid=11IuAOf150Ws2yDVmDdJcPCKR9NsC2ChE

This report documents the results and preliminary interpretation on samples submitted to the NAM project by the Geological Survey of South Australia.

South Australian samples analysed in the NAM cover three sub-project areas (Fig. 1; Table 1):

1. Olympic Cu-Au Province, eastern Gawler Craton
2. Cairn Hill Fe-Cu deposit and vicinity, northern Gawler Craton
3. Curnamona Province

This report describes the results from the first two of these. A second report covers the results of the Curnamona Province analyses and includes results from samples from the New South Wales portion of the Curnamona Province collected in collaboration with the Geological Survey of New South Wales.

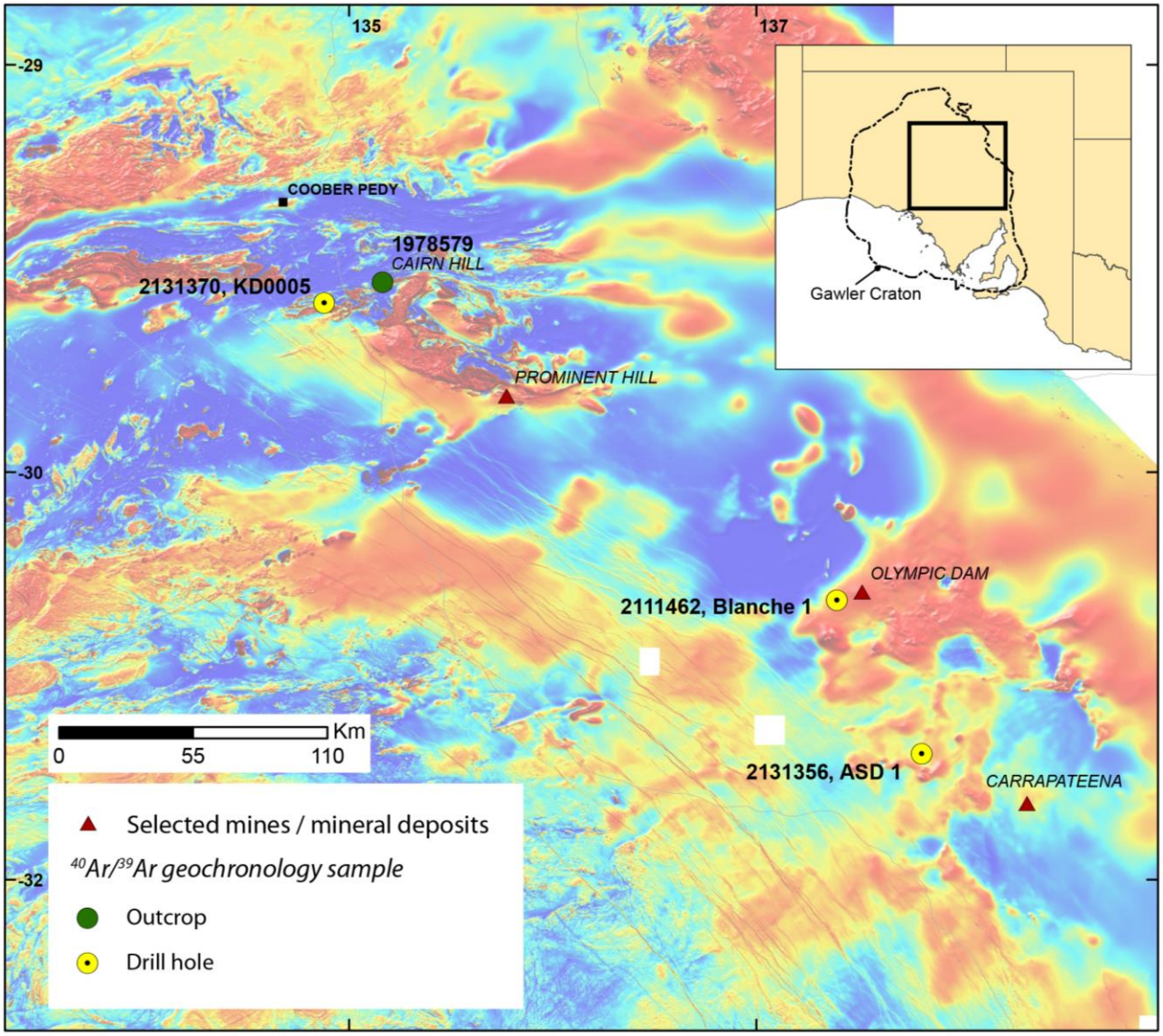

Figure 1. Location of samples described in this report. Samples are listed as either outcrop or drill hole samples, with the sample number and drill hole name also indicated on the map. Selected mines and mineral deposits are shown for reference. Background geophysical image is an overlay of South Australian reduced to pole total magnetic intensity image from the Gawler Craton Airborne Survey (available via SARIG, https://map.sarig.sa.gov.au/). Inset shows location of the map with respect to the Gawler Craton and state borders of South Australia.

Table 1. Summary of samples described in this report

Sample	Lithology	Location	Dated mineral	Drill hole	DH No.	Depth-from	Depth-to	Dlat	Dlong
2131356	altered granite	Olympic Cu-Au Province	muscovite	ASD 1	20722	960.45	962.4	-31.0365	137.1089
2111462	altered granite	Olympic Cu-Au Province	K-feldspar	Blanche 1	206086	1005.6	1006	-30.4701	136.7971
1978579	altered granite	Cairn Hill mine	hornblende, K-feldspar					-29.2999	135.1227
2131370	felsic gneiss	near Cairn Hill	biotite, K-feldspar	KD0005	215245	130.5	131.9	-29.3758	134.9083

ANALYTICAL PROCEDURES: ^{40}AR/^{39}AR GEOCHRONOLOGY

Samples were selected from drill core and legacy outcrop samples and subject to standard crushing, sieving and density separation techniques to separate the alkali feldspar minerals. Mineral separation was conducted at the Research School of Earth Sciences, Australian National University. Samples were then handpicked to >99% purity, wrapped in aluminium foil, inserted into a canister with appropriate standards and other material used to determine correction factors, and submitted for irradiation. ^{40}Ar/^{39}Ar geochronology was conducted at the Research School of Earth Sciences, Australian National University, Canberra using methodology and instrumentation identical to that described in detail in Forster et al. (2010), Forster et al. (2015) and Pownall et al. (2017).

Briefly, samples were irradiated in two separate batches alongside CaF_2 and K-glass standards and irradiated at UC Davies nuclear reactor, USA, for 12 hours and 5 minutes along with flux monitors, K_2SO_4, and CaF_2 salts for calculation of J factors, and monitoring correction factors including ^{40}Ar production from potassium. Biotite standard GA-1550 (98.5 ± 0.8 Ma K–Ar age; Spell and McDougall, 2003) was used as the flux monitor. Analyses were conducted via a furnace step-heating procedure through an ultrahigh-vacuum extraction line to a VG1200 gas-source mass spectrometer, with abundances of ^{36}Ar, ^{37}Ar, ^{38}Ar, ^{39}Ar, and ^{40}Ar measured with a 7.6×10^{-17} mol mV^{-1} sensitivity. Flux monitors were degassed using a Coherent infrared diode laser and analysed using the same extraction line and mass spectrometer. Step heating diffusion experiments on individual samples were carried out with a temperature-controlled furnace that allows precise control of temperature during step-heating, with schedules of 34 to 36 heating steps between 450 °C and 1450 °C. Step-heating experiments for K-feldspar samples involved a minimum of two separate isothermal steps before the next sequence of isothermal steps was commenced, with peak temperature typically increased by >30–50 °C for each isothermal sequence. This was undertaken in order to minimize the effect of contaminating excess argon (Lovera et al., 1997).

Data were reduced using Noble v1.8 software using the correction factors and J-factors listed in Appendix 1. ^{40}K abundances and decay constants are those recommended by Renne et al. (2011). Age spectra and other isotope plots were constructed using *eArgon* software.

Ages were derived from the age spectra based on the method of asymptotes and limits (Forster and Lister, 2004). Complex age spectra result from mixtures between different age components within the sample. The key point of recognising limits within the age spectra is that analysis of age spectra using asymptotes and limits enables maximum and minimum constraints to be placed on the timing of the various events that the rock has been subjected to (Forster and Lister, 2004). The mixtures of ages that complex age spectra record can preserve, or partially preserve, information on the timing of episodes of microstructural, thermal or metasomatic processes in the mineral analysed. A detailed description of methodologies is given in Muston et al. (2021).

RESULTS

OLYMPIC CU-AU PROVINCE

The Olympic Cu-Au Province is a metallogenic province in South Australia that contains one of the world's most significant Cu-Au-U resources in the Olympic Dam deposit. The Olympic Cu-Au Province also hosts a range of other iron oxide-copper-gold (ICOG) deposits including the Prominent Hill and Carrapateena deposits (Skirrow et al., 2007; Skirrow, 2010; Reid, 2019).

Previous thermochronology work within the region of the Olympic Dam deposit has demonstrated that the mineralising event at c. 1590 Ma is also recorded as a thermal event in biotite and muscovite in some country rocks of the region (Skirrow et al., 2007). The Olympic Dam deposit is hosted within c. 1595 Ma granite of the Hiltaba Suite (Ehrig et al., 2012; Cherry et al., 2018; Courtney-Davies et al., 2020).

To the north east of Olympic Dam, $^{40}Ar/^{39}Ar$ dating of hydrothermal K-feldspar suggests that younger events have also modified the crust in this region, with evidence for c. 1.3 – 1.1 Ga fluid flow (Reid et al., 2017). Dating of apatite by laser ablation U-Pb methods yields a range of ages across the region from c. 1.9 Ga to c. 1.2 Ga (Hall et al., 2018). Given the sparsity of data, the thermal evolution of the Olympic Cu-Au Province is poorly constrained and the influence of younger events poorly known.

The first sample dated in this National Argon Map sample is an altered granite in the vicinity of the Oak Dam prospect, drill hole ASD 1. The second is a hematite altered Hiltaba Suite granite in the vicinity of Olympic Dam, drill hole Blanche 1 (Fig. 2).

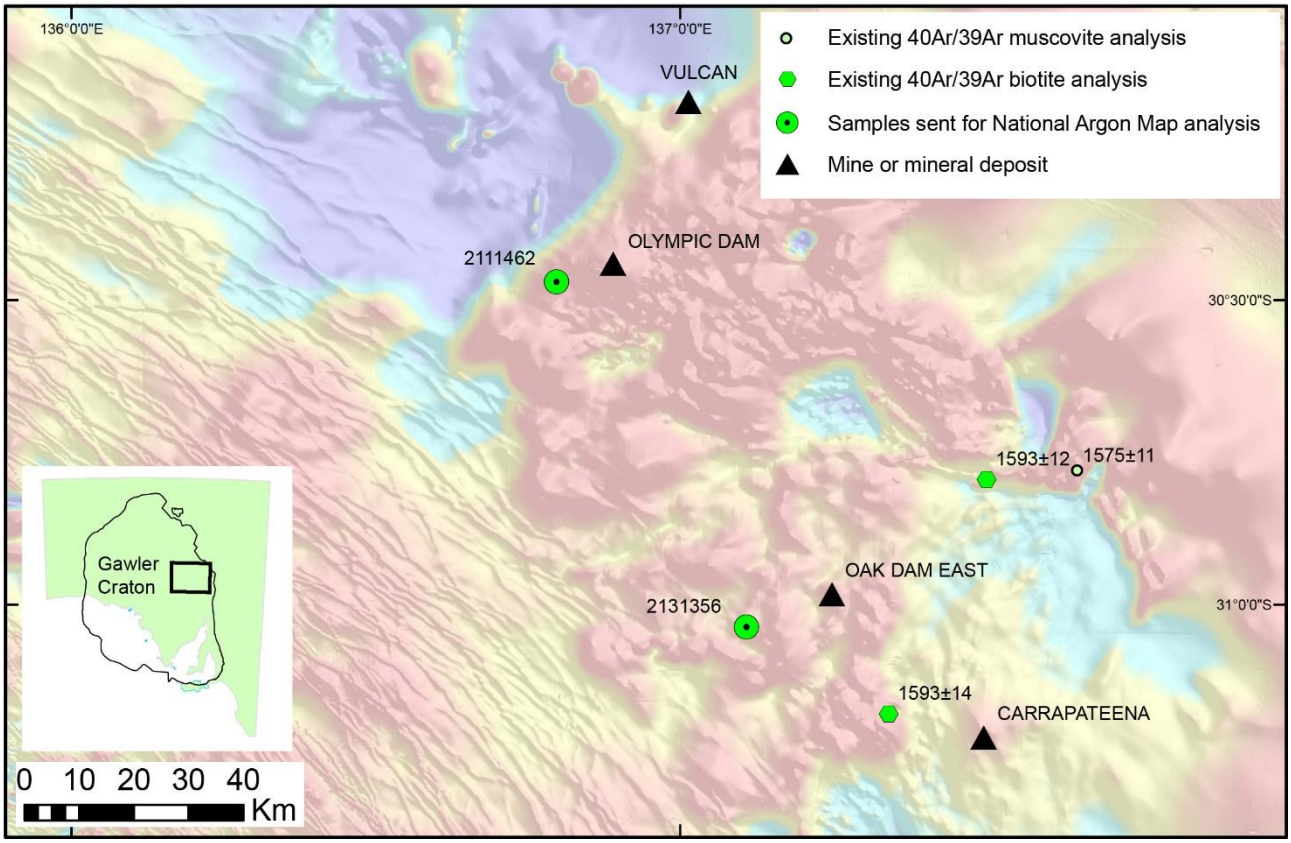

Figure 2. Location of samples in the Olympic Dam region analysed as part of the National Argon Map along with previous samples dated by Skirrow et al. (2007). Ages given are plateau ages from each biotite or muscovite analysis.

2131356: altered granite, drill hole ASD 1

Sample	**2131356**		
Collector:	A. Reid		
Location GDA2020:	701269.78	6564445.28	Zone 53
Location Lat-Long:	-31.0364764	137.1088647	
250K map sheet:	SH5316 TORRENS		
100K map sheet:	6335 Arcoona		
Location:	Drill hole ASD 1, 960.45 - 962.4m		
Mineral analysed	**muscovite**		
Date analysed:	13/Nov/2020		
Interpreted age:	c. 952.8		
Age type:	Upper limit in age spectrum		
Age interpretation:	Minimum age of oldest growth/resetting		
Interpreted age:	c. 496.6 Ma		
Age interpretation:	Lower limit in age spectrum		
Age interpretation:	Maximum age for youngest growth/resetting event		

BACKGROUND

Sample 2131356 is an altered granite from drill hole ASD 1 (Fig. 3). The granite is hematite altered and the muscovite is medium to fine grained. The analysis of muscovite may provide constraints as to the timing of the alteration in the region to the east of Oak Dam. Oak Dam West is a major new discovery by BHP in the region. The granite is part of the c. 1850 Ma Donington Suite. Apatite laser ablation-inductively coupled plasma mass spectrometry (LA-ICPMS) U-Pb analysis on this sample yielded an age of $^{206}Pb/^{238}U$ age of 1811 ± 26 Ma (MSWD = 1.2) (Hall et al., 2018), suggesting the rock is part of the c. 1850 Ma Donington Suite.

Figure 3. Photograph of sample 2131356.

PETROGRAPHY

Sample 2131356 is an altered granite (Fig. 4). The quartz-feldspar texture is granoblastic with extensively altered feldspar. The quartz grains have irregular grain boundaries that appear corroded, with some evidence for sub-grain development. The feldspar is pervasively replaced with white mica and or chlorite. There are knots of coarse white mica (muscovite) that appear to overgrow the main granoblastic texture. These white mica knots have relatively low birefringence and appear ragged, possibly partly replaced by chlorite.

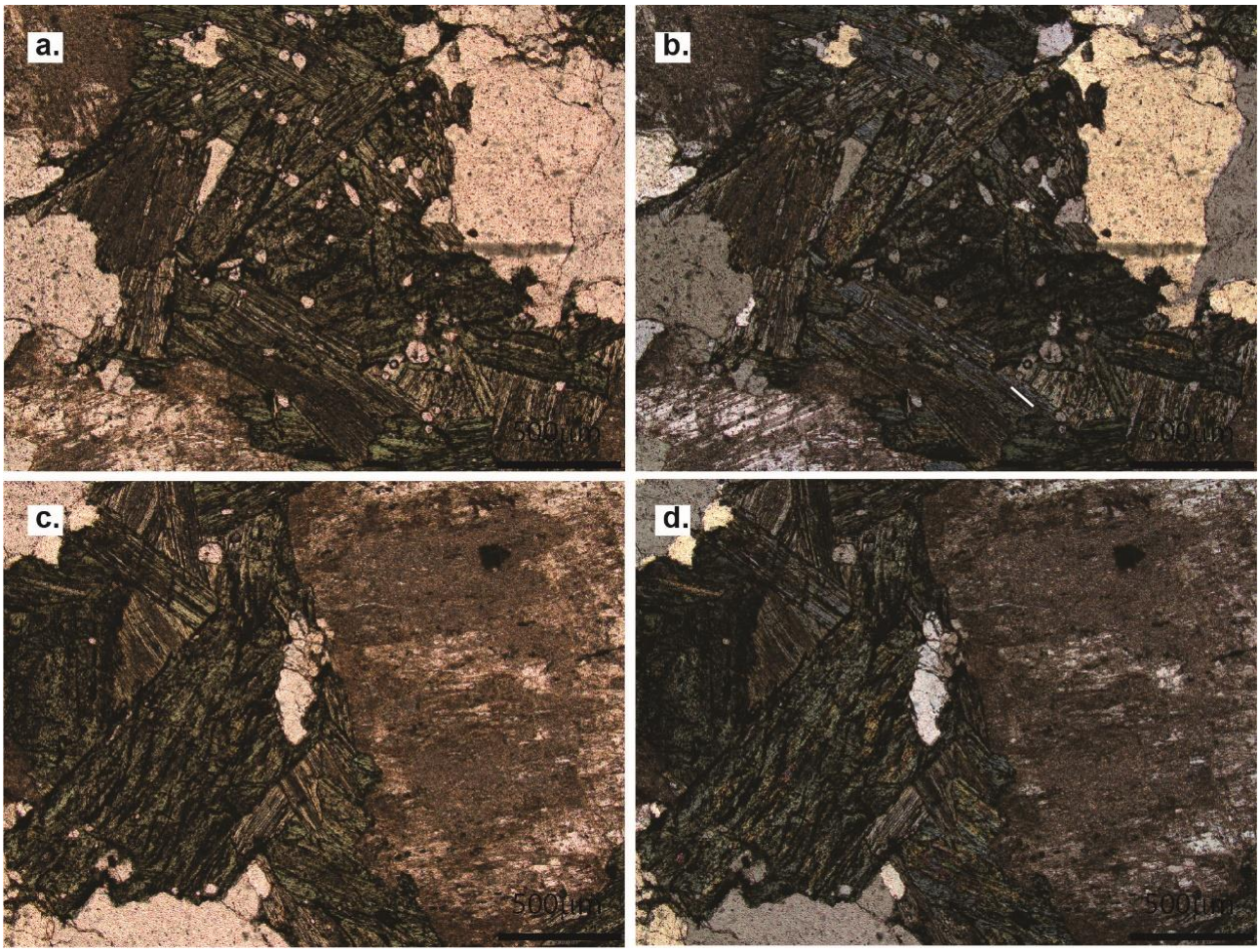

Figure 4. Thin section photomicrograph of sample 2131356, drill hole ASD 1. Plain polarised light on left, cross polars on right. 2.5x magnification. **(a-b)** Coarse chlorite-altered muscovite and partly resorbed quartz. **(c-d)** Chlorite altered muscovite adjacent large, altered K-feldspar.

RESULTS

The $^{40}Ar/^{39}Ar$ age spectra for muscovite from sample 2131356 is highly disturbed (Fig. 5a). The lower age limit is c. 496.6 Ma at ~10% ^{39}Ar released and an upper age limit occurs at c. 952.8 Ma at step 12 at around 80% ^{39}Ar released. The age spectra is dominated by mixing between these two limits. After step 16, the remaining ~7% ^{39}Ar released shows extreme discordance, with very high uncertainties.

The isotope correlation diagram for sample 2131356 reveals there is a significant component of non-radiogenic ^{39}Ar in the mineral analysed, with the steps having $^{36}Ar/^{40}Ar$ ratios around 0.002 (Fig. 5b). This is also reflected in the percentage of radiogenic ^{40}Ar plot (Fig. 5c). The Ca/K and Cl/K ratios indicate that the final steps in the age spectra are strongly influenced by both Ca and Cl and are likely not geologically meaningful (Figs 5e, d).

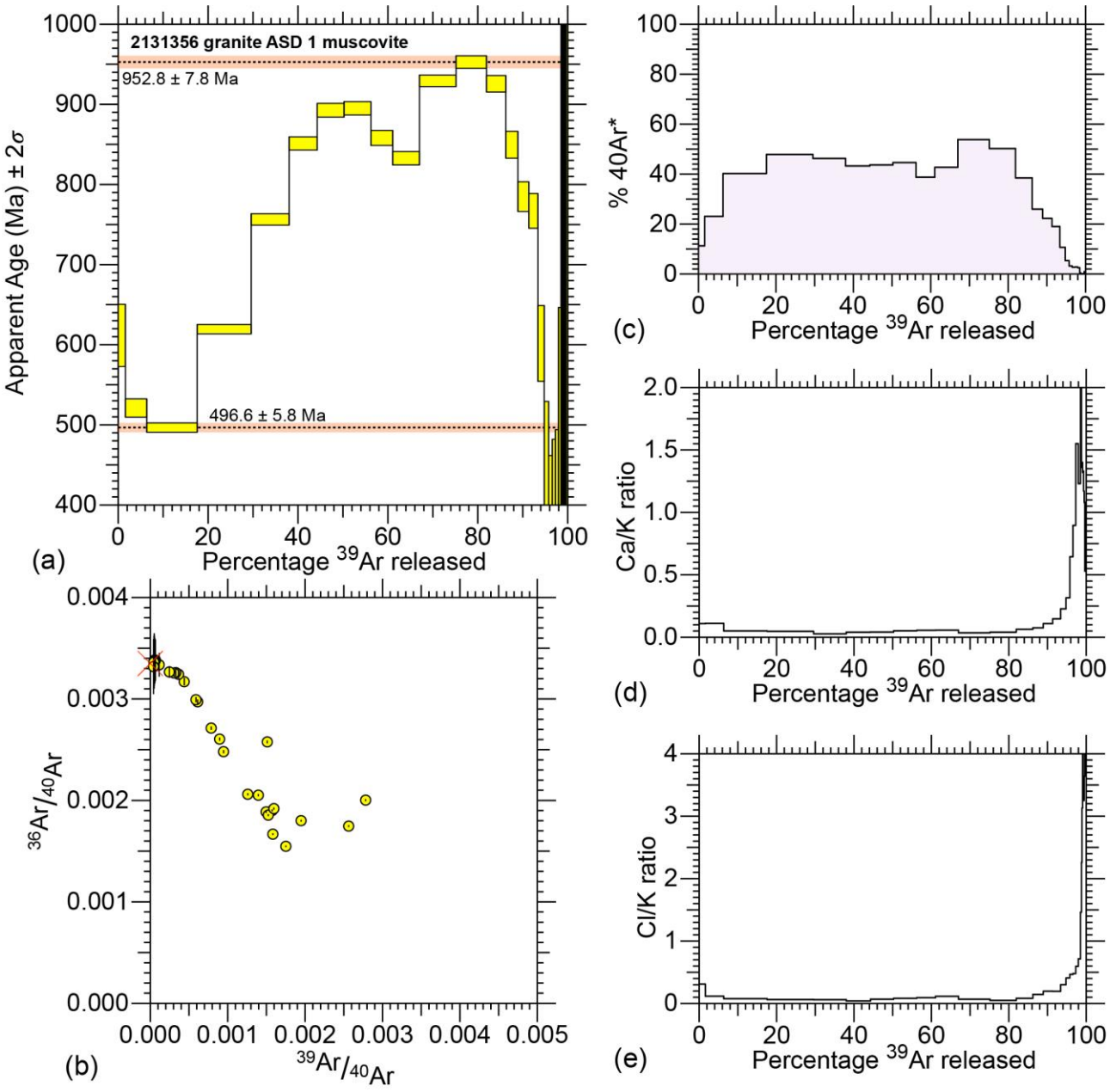

ANU CAN #36, Name: 2131356, Foil: A01, Mineral: Muscovite, Mass: 3.1mg, Steps: 30
Australia; SA; Eastern Gawler Craton; Altered granite; Grain Size: 420-250µm
Age 952.8 ± 7.8 Ma (95% c.l) Selected step(s): 12
Age 496.6 ± 5.8 Ma (95% c.l) Selected step(s): 3

Figure 5. Analytical results for sample 2131356 (a) age spectrum, (b) isotope correlation diagram, (c) percentage radiogenic ^{40}Ar ($^{40}Ar^*$), (d) Ca/K ratio, and (e) Cl/K ratio.

GEOCHRONOLOGICAL INTERPRETATION

Petrologically mica appears to be late, overprinting earlier magmatic minerals such as quartz and feldspar. The feldspar is highly altered. The age spectra from muscovite in sample 2131356 is highly discordant and suggests mixing between populations with ages between c. 499 Ma and c. 956 Ma. The geological significance of these results is difficult to assess, but a possible interpretation is that the mica originally grew in the Neoproterozoic as an alteration mineral, and subsequently modified by further alteration during the Cambrian.

2111462: altered granite, drill hole Blanche 1

Sample	**2111462**		
Collector:	A. Reid		
Location GDA2020:	672516.76	6627750.51	Zone 53
Location Lat-Long:	-30.4700925	136.797095	
250K map sheet:	SH5312 ANDAMOOKA		
100K map sheet:	6237 Mattaweara		
Location:	Drill hole Blanche 1, 1005.6 - 1006 m		
Mineral analysed:	**K-feldspar**		
Date analysed:	17/Nov/2020		
Interpreted age:	1500.6 ± 9.2 Ma		
Age type:	Upper age limit		
Age interpretation:	Cooling age		
Interpreted age:	1153.7 ± 4.2 Ma.		
Age type:	Intermediate age limit		
Age interpretation:	Hydrothermal alteration		
Interpreted age:	1406.2 ± 5.7 Ma		
Age type:	Intermediate age limit		
Age interpretation:	Hydrothermal alteration		
Interpreted age:	c. 682.8 Ma		
Age type:	Lower age limit		
Age interpretation:	Hydrothermal alteration		

BACKGROUND

Sample 211462 is a coarse-grained granite from geothermal drill hole Blanche 1 (Fig. 6; Meyer, 2006). The granite comprises syenogranite and monzogranite, generally massive but with several zones of low- and high-angle fractures. This drill hole site is located about 8 km southwest of Olympic Dam near the western edge of the Roxby Downs Granite, which also hosts the Olympic Dam Cu-U-Au deposit, and forms part of the Burgoyne Batholith. The Burgoyne Batholith is overlain by platform sedimentary rocks of the Stuart Shelf.

A high precision chemical abrasion-thermal ionisation mass spectrometry (CA-TIMS) zircon age from sample 2111460 from this same drill hole (depth 1563.1–1564.6 m) yields a crystallisation age of 1591.79 ± 0.42 Ma for the granite (Jagodzinski et al., 2021).

Hall et al. (2018) analysed apatite via U-Pb and fission track methods, obtaining a weighted mean $^{206}Pb/^{238}U$ age of 1559 ± 20 Ma (MSWD = 0.53), calculated from 24 apatite analyses. Sample 2111462 recorded an AFT central age of 207 ± 21 Ma (Hall et al. 2018).

Figure 6. Photograph of sample 2111462.

PETROGRAPHY

Sample 211462 is an altered coarse-grained, syenogranite with red feldspars, chloritised biotite, and minor hornblende. The quartz grains are rounded or resorbed and also occur as interstitial films, which suggests shallow level of emplacement. K-feldspar in this sample is largely euhedral to subhedral microcline with cross-hatch twinning and perthitic lamellae (Fig. 7). Rapakivi texture is also present in several grains, with the alkali feldspar overgrown by a rim of plagioclase. Microcline also displays albite alteration along microstructural lamellae and intragranular fracture zones. These albite patches are also associated with sericite and carbonate (dolomite) that occurs as patchy zones within individual microcline crystals. The red colouration of the microcline, is likely a result of micron-scale hematite inclusions

Biotite is present as relict patches within chlorite-epidote-carbonate clots. Trace titanite, ilmenite, apatite and fluorite, occurring as either relict primary minerals or due to alteration. Pyrrhotite and sphalterite are present along with patches of hematite. Micro-cracks are filled with chlorite-carbonate-biotite.

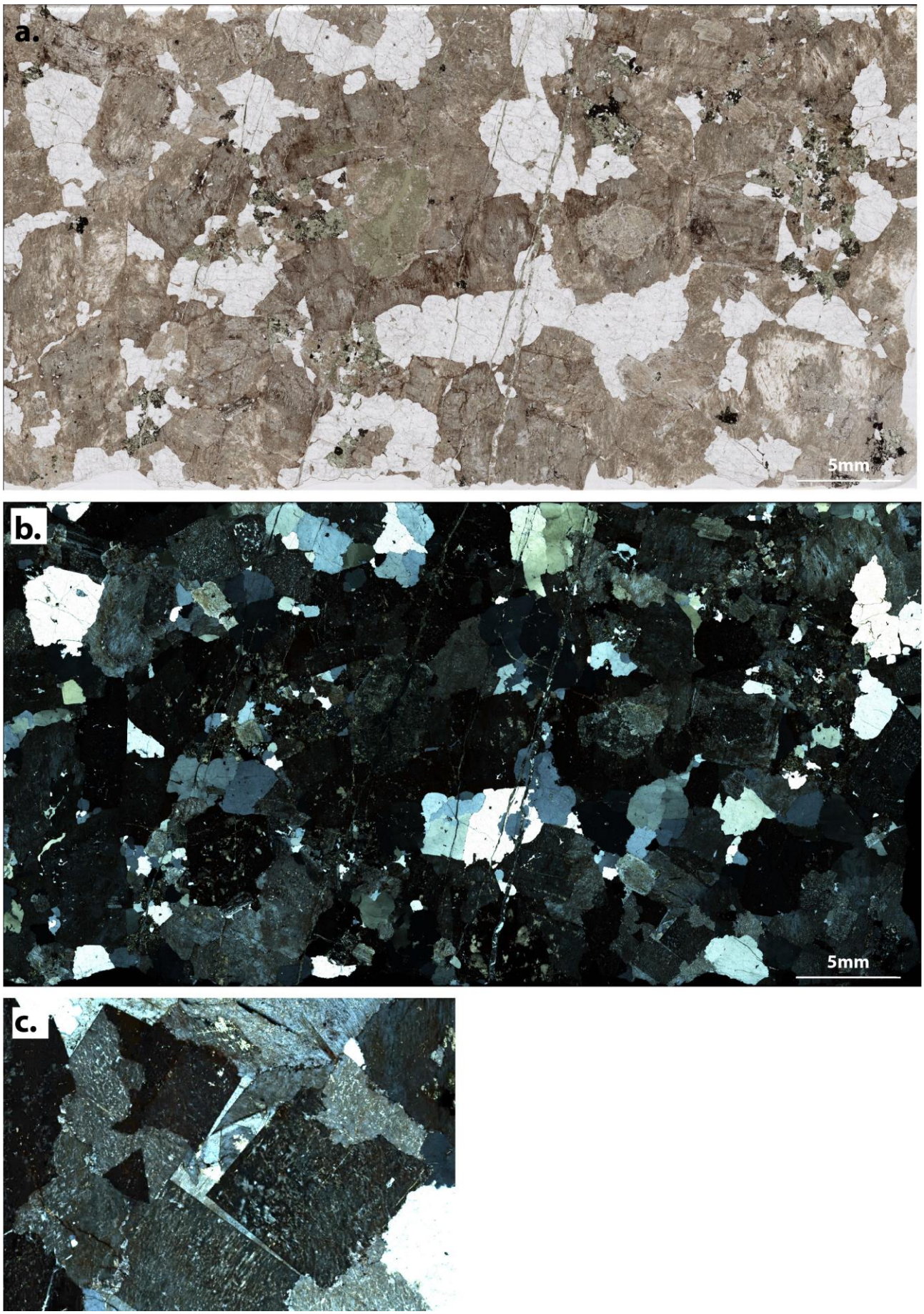

Figure 7. Thin section photomicrograph of sample 211462, drill hole Blanche 1. **(a)** Transmitted plain light. **(b)** Cross polars. **(c)** Detail of euhedral K-feldspar and interstitial quartz. Cross polars.

RESULTS

The $^{40}Ar/^{39}Ar$ age spectrum for K-feldspar sample 2111462 is a complex spectrum with several components (Fig. 8a). The initial 10% gas released shows a range of high to geologically unreasonable ages, likely the result of excess ^{40}Ar, potentially present in fluid inclusions related to the extensive alteration in this sample. No geological significance is attached to the ages in this portion of the spectrum.

The age spectrum has a minimum age of c. 682.8 Ma, represented by step 18. From this point the age steps upwards to an intermediate grouping, represented by a group of three steps (28, 29 and 30) which can be averaged to yield an age of 1153.7 ± 4.2 Ma.

Subsequent to this the age spectrum again climbs to a second age cluster at around 1406.2 ± 5.7 Ma, an average of the ages for steps 34 and 35. The final portion of the spectrum reaches maximum ages of 1500.6 ± 9.2 Ma, defined by step 39. This age is the upper age limit for K-feldspar in this sample.

The isotope correlation diagram shows clusters of steps, some with elevated non-radiogenic argon, but the majority of which cluster towards very low $^{36}Ar/^{40}Ar$ values (Fig. 8b). Radiogenic ^{40}Ar fluctuates considerably in the early heating steps and then increases to between 80 and 90 % for the majority of steps (Fig. 8c). Both the Ca/K and Cl/K ratios are elevated in the first 10% gas release corresponding to elevated ages (Fig. 8d, e). This supports the notion that this portion of the age spectrum is a consequence of alteration, rather than recovery of geologically meaningful ages.

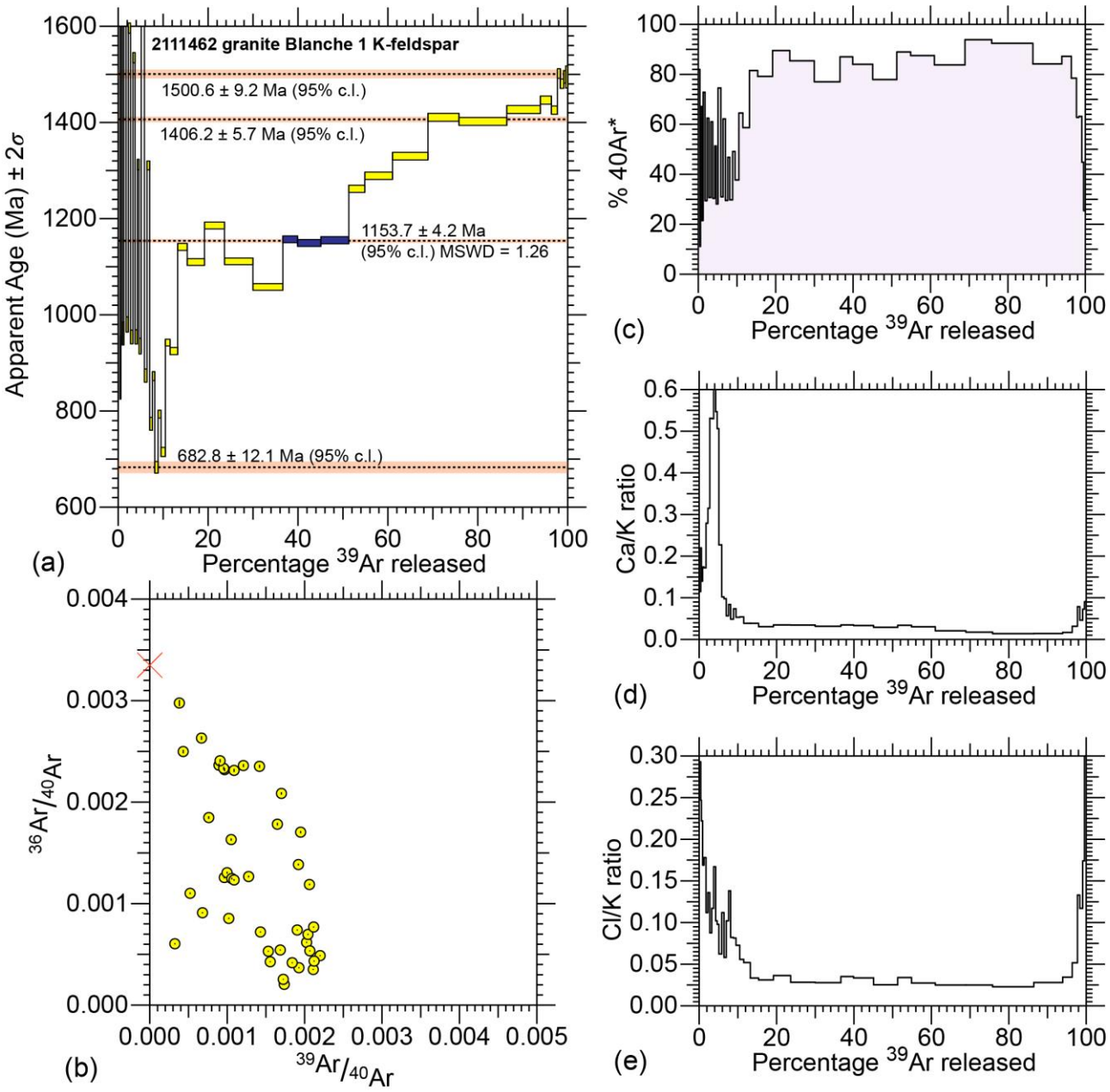

ANU CAN #36, Name: 2111462, Foil: A02, Mineral: K-Feldspar Fine, Mass: 4.6mg, Steps: 42
Australia; SA; Eastern Gawler Craton; Altered granite; Grain Size: 420-250µm
Age 1500.6 ± 9.2 Ma (95% c.l) Selected step(s): 39 42
Age 1406.2 ± 5.7 Ma (95% c.l) Selected step(s): 34 35
Age 1153.7 ± 4.1 Ma (95% c.l) Selected step(s): 28 29 30
Age 682.8 ± 12.10 Ma (95% c.l) Selected step(s): 18

Figure 8. Analytical results for sample 2111462 (a) age spectrum, (b) isotope correlation diagram, (c) percentage radiogenic ^{40}Ar ($^{40}Ar^*$), (d) Ca/K ratio, and (e) Cl/K ratio.

GEOCHRONOLOGICAL INTERPRETATION

The age spectrum from sample 2111462 suggests multiple phases of geological activity are recorded in the K-feldspar. Initial cooling is recorded as early as c. 1500 Ma, which may reflectthe timing of a post-magmatic fluid event. The c. 1406 Ma age cluster may potentially be related to geological processes such as deposition of the overlying Pandurra Formation in the region (Beyer et al., 2018).

The c. 1154 Ma age cluster may reflect new mineral growth or resetting due to thermal or metasomatic events related to the Musgravian-aged tectonic activity that is widespread across central Australia (the Musgrave Orogen). Ages similar to this were recorded in adularia from drill hole DP-1, to the north-west of Olympic Dam (Reid et al., 2017).

Finally, the younger age limit at c. 683 Ma is very similar to the timing of deposition of the overlying Neoproterozoic rocks of the Stuart Shelf. Potentially basin fluids have percolated into the underlying basement and modified the age profile within the K-feldspar of this sample.

CAIRN HILL FE-CU DEPOSIT AND VICINITY, NORTHERN GAWLER CRATON

The Cairn Hill Fe-Cu deposit is an example of magnetite-dominant iron oxide copper gold (IOCG) mineralisation in the Gawler Craton. Hematite-dominant IOCG deposits are well represented within the Olympic Cu-Au Province, including Olympic Dam, Prominent Hill and Carrapateena (Skirrow et al., 2007).

The Cairn Hill deposit is located on a west-east trending magnetic body along the northern edge of the Mount Woods Domain that can be traced for over 15 km strike length. The orebody itself comprises two sub parallel magnetite lodes with ore grades approximately 62% Fe and 1.2% Cu. The wall rock to both lodes is foliated, quartzofeldspathic granite gneiss. The quartzofeldspathic granite gneiss at Cairn Hill crystallised at 1572 ± 6 Ma and is interpreted to be part of the Hiltaba Suite (Jagodzinski and Reid, 2015). Apatite within garnet-apatite-magnetite alteration yielded a U-Pb age of 1466 ± 5 Ma (sample 2013956).

$^{40}Ar/^{39}Ar$ geochronology from the Cairn Hill deposit has been previously undertaken (see Jagodzinski and Reid, 2015). One of the aims of the present study was to improve the results of the previous $^{40}Ar/^{39}Ar$ dating undertaken using laser ablation instrumentation. The previous hornblende analysis resulted in outgassing in a small number of heating steps, with a consequently highly imprecise age profile.

1978579: magnetite-amphibole altered quartzofeldspathic granite gneiss, Cairn Hill Mine

Sample	**1978579**		
Collector:	A. Reid		
Location GDA2020:	511919.52	6758776.47	Zone 53
Location Lat-Long:	-29.2999413	135.122733	
250K map sheet:	SH5307 BILLA KALINA		
100K map sheet:	5939 Engenina		
Location:	Mine rock sample, Cairn Hill mine, Pit 1; south face of decline, RL 93.129m		
Mineral analysed:	**hornblende**		
Date analysed:	03/Dec/2020		
Interpreted age:	1412.5 ± 3.7 Ma		
Age type:	Plateau age		
Age interpretation:	Hydrothermal alteration		
Mineral analysed:	**K-feldspar**		
Date analysed:	05/Dec/2020		
Interpreted age:	1278.9 ± 6.7 Ma		
Age type:	Upper age limit		
Age interpretation:	Cooling age?		
Interpreted age:	995.0 ± 6.6 Ma		
Age type:	Lower age limit		
Age interpretation:	Cooling age?		

BACKGROUND

Sample 1978579 is a foliated leucogranite that is the dominant host rock to the magnetite orebody and was sampled on the southern wall of the decline into the Cairn Hill pit. The sample comprises monzogranite with an abundance of mm to cm scale magnetite-amphibole-biotite ± hematite ± sulphide veins (Fig. 9). These veins are interpreted to be related to the massive magnetite ore zones that make up the deposit.

Figure 9. Photograph of sample 1978579. The coarse-grained amphibole-magnetite alteration cuts the pre-existing granitic fabric and is also associated with sericitisation of feldspar (plagioclase). Note: hornblende from this sample is from within the alteration vein. K-feldspar was sampled taken away from the obvious light-coloured white mica (sericite) alteration.

PETROGRAPHY

Sample 1978579 is a foliated medium-grained granite. The mafic vein that cuts the granite contains coarse grained hornblende intergrown with magnetite and minor apatite, with hornblende preserving very few inclusions (Fig. 10).

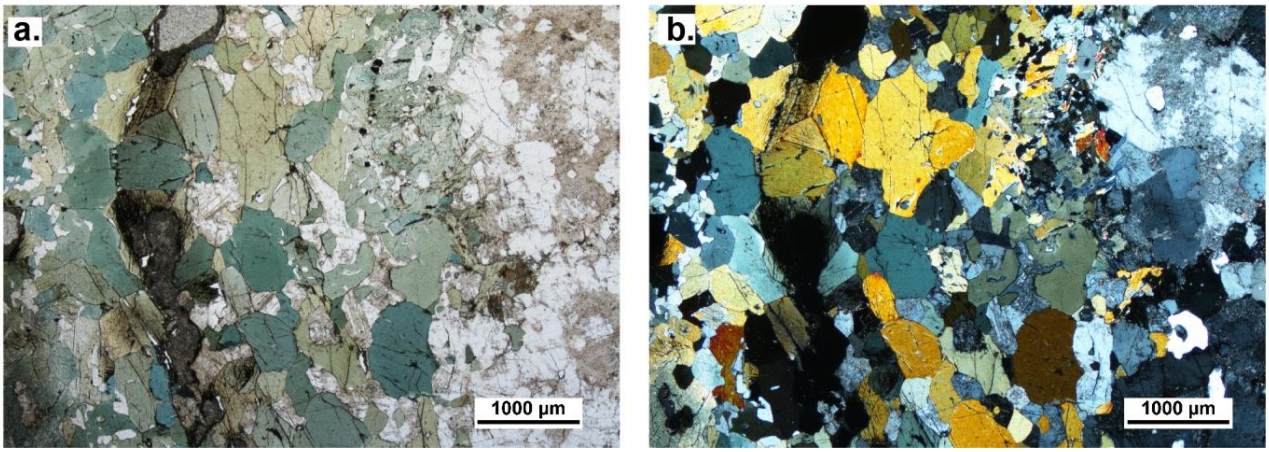

Figure 10. Photomicrographs of sample 1978579. (a) Plain polarised light. **(b)** Cross polars. Photographs show the transition from the hornblende-rich magnetite-bearing alteration on the left of the field of view to the quartz and sericite altered feldspar that represents the granite on the right.

RESULTS

Hornblende

The $^{40}Ar/^{39}Ar$ age spectrum for hornblende from sample 1978579 is very simple, with steps 15, 16, 17, 18, 19, 20, 23, 24, 25, 26 and being able to be combined for a weighted mean age of 1410 ± 2.6 Ma (Fig. 11a). The simplicity of the age spectrum is reflected in the simple array on isotope correlation diagram from which an isochron age of 1402.7 ± 1.4 Ma can be calculated (Fig. 11b). This is also reflected in the flat $^{40}Ar^*$, Ca/K and Cl/K profiles (Fig. 11b, c, d, e).

K-feldspar

The first ~10% gas released from the $^{40}Ar/^{39}Ar$ age spectrum for K-feldspar from sample 1978579 contains age variations that include geologically unreasonable ages derived from excess ^{40}Ar (Fig. 12a). The remaining portion of the spectrum steps upwards from a minimum of 991.5 ± 6.8 Ma towards a maximum age of 1274.8 ± 7.7 Ma.

The isotope correlation diagram shows the majority of steps cluster towards very low atmospheric component, which is also reflected in the relatively high $^{40}Ar^*$ values for the majority of the experiment (Fig. 12b, c). The Cl/K and Ca/K ratios also suggest the first portion of the age spectrum is a result of variation in composition, possibly as a result of fluid inclusions or chlorite/sericite intergrowths within the K-feldspar (Fig. 12d, e).

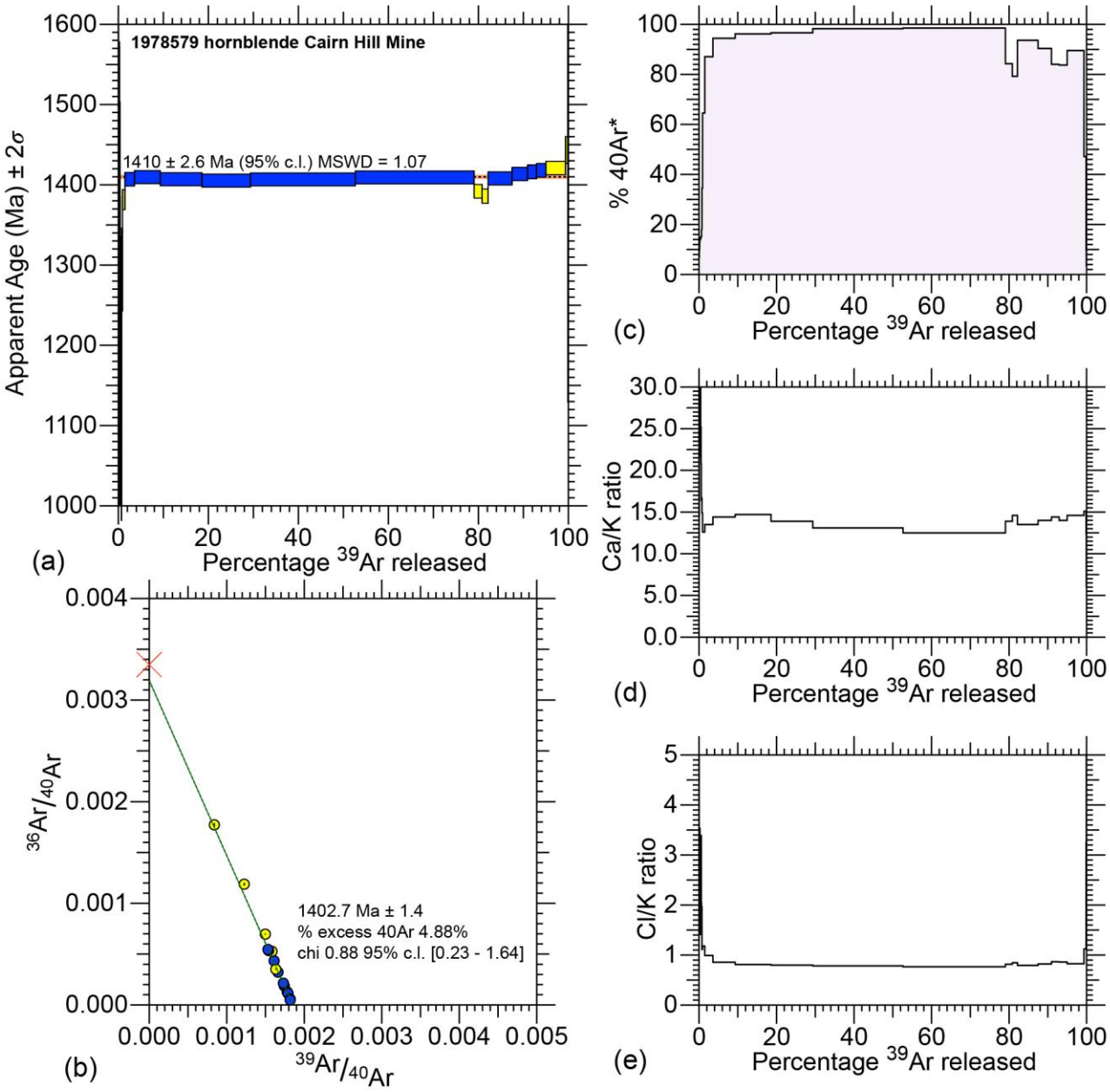

ANU CAN #36, Name: 1978579, Foil: A06, Mineral: Hornblende, Mass: 30.6mg, Steps: 30
Australia; SA; Cairn Hill mine; Altered granite; Grain Size: 420-250µm
Age 1410 ± 2.6 Ma (95% c.l) Selected step(s): 15 16 17 18 19 20 23 24 25 26
Pearson's chi statistic 1.04 with 95% confidence range f=9 [0.25 - 1.63].
Age based on selected steps 1410 ± 2.6 Ma (95% c.l.) MSWD = 1.07

There is 1 stored line on the Turner Inverse Ar40 correlation plot
Selected steps: 15 16 17 18 19 20 23 24 25 26
Y-axis 40Ar/36Ar ratio 313.132 ± 1.6%
Age determined using x-axis intercept 1402.7 Ma ± 1.02E-01 %
Excess 40Ar 4.9%

The chi-statistic uses formulae in Wendt and Carl 1991. MSWD = 0.780. Pearson's chi statistic (sqrt MSWD) is 0.88 with the 95% confidence range [0.23 - 1.64] for 8 degrees of freedom. Chi is -0.15 from the most likely expected value = 0.935 ± 0.351, so the observed scatter is within the tolerance of that to be expected for a single age.

Figure 11. Analytical results for hornblende of sample 1978579 (a) age spectrum, (b) isotope correlation diagram, (c) percentage radiogenic ^{40}Ar ($^{40}Ar^*$), (d) Ca/K ratio, and (e) Cl/K ratio.

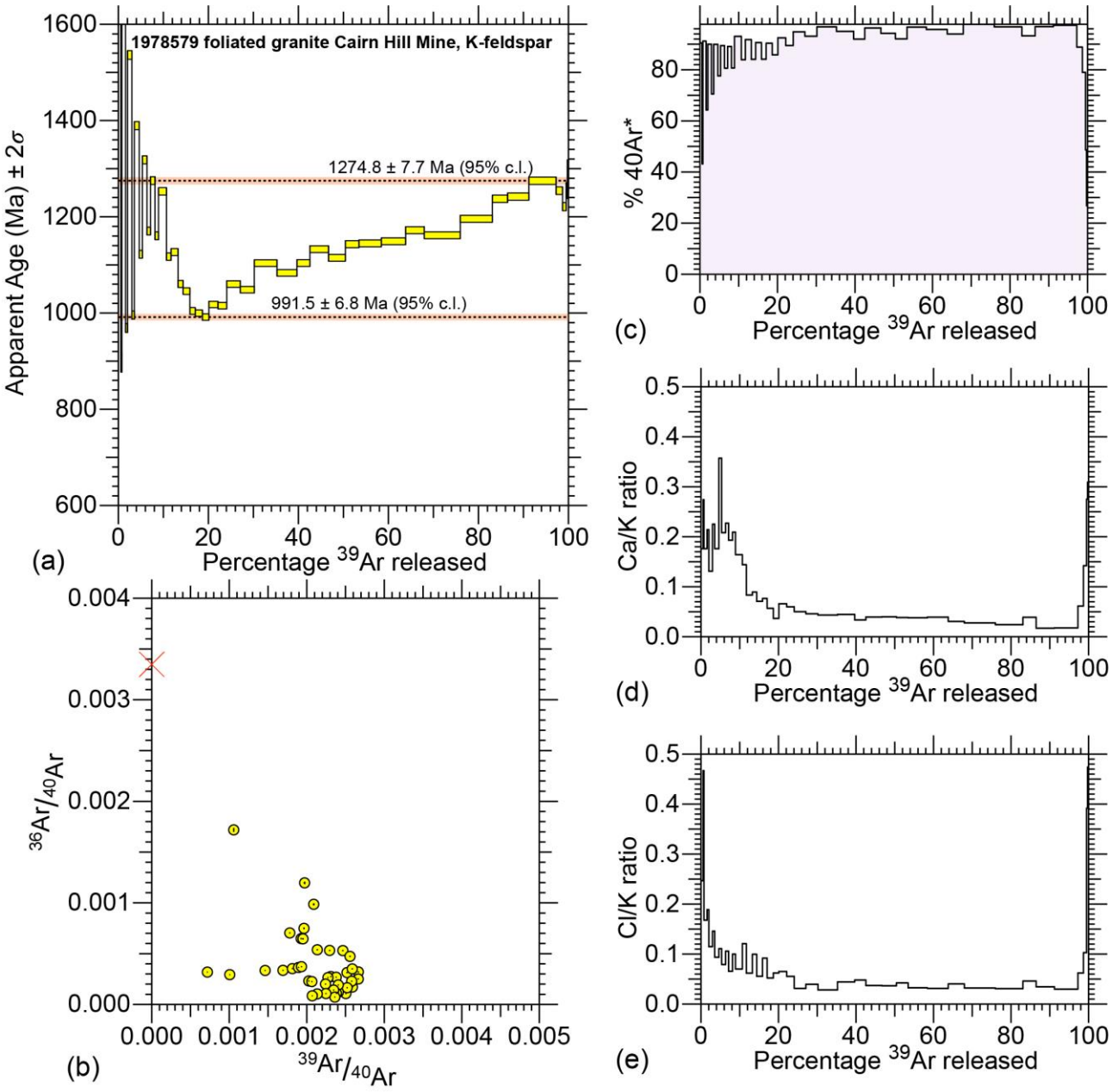

ANU CAN #36, Name: 1978579, Foil: A08, Mineral: K-Feldspar Fine, Mass: 4.3mg, Steps: 42
Australia; SA; Cairn Hill mine; Altered granite; Grain Size: 420-250µm
Age 1274.8 ± 7.7 Ma (95% c.l) Selected step(s): 38
Age 991.5 ± 6.8 Ma (95% c.l) Selected step(s): 20

Figure 12. Analytical results for K-feldspar of sample 1978579 (a) age spectrum, (b) isotope correlation diagram, (c) percentage radiogenic ^{40}Ar ($^{40}Ar^*$), (d) Ca/K ratio, and (e) Cl/K ratio.

GEOCHRONOLOGICAL INTERPRETATION

The $^{40}Ar/^{39}Ar$ data for hornblende within the hornblende-magnetite vein in this sample is consistent with rapidly cooled sample, as the age spectrum is essentially flat, and there is a single age population recorded. If subsequent heating events were of prolonged duration or the entire sample was subject to prolonged residence at high temperature then the age spectrum is likely to show a decrease towards younger ages in the early part of the heating schedule, however this is not observed. The data can be interpreted as either demonstrating the vein was formed at 1412 ± 2.6 Ma during a hydrothermal event that crystallised hornblende and magnetite, or that the entire sample was subject to significant heating at this time and produced a resetting of the argon age profile within the hornblende. The first of these options is geologically simpler to envisage.

Further work is required to compare this data to other isotopic constraints on the timing of mineralisation at Cairn Hill. For example, previous laser induced step heating $^{40}Ar/^{39}Ar$ data from this same sample yielded an age of 1492 ± 6 Ma (Jagodzinski and Reid, 2015). It may be that there are implications for methodological approaches to argon dating that can be gained by comparing these two results. A discussion of this is beyond the scope of this report.

Furthermore, previous U-Pb apatite data from Cairn Hill suggests apatite-bearing magnetite-pyroxene alteration occurred at 1466 ± 5 Ma (Jagodzinski and Reid, 2015). This data may suggest that there were multiple episodes of alteration that are recorded by the different minerals of the deposit. Further work is required to examine the variation in age from different geochronometers.

The K-feldspar data from this sample yields considerably younger ages than the hornblende from the vein. This suggests thermal or microstructural recrystallisation has affected the K-feldspar but not the hornblende. The oldest ages in the K-feldspar suggest a thermal or microstructural event occurred at or prior to c. 1274.8 Ma. A lower limit on the timing of final cooling is given by the age c. 991.5 Ma. Further work on the microstructural history of this sample, including interrogation of the Arrhenius data from the $^{40}Ar/^{39}Ar$ analysis may indicate the temperature conditions required to have occurred for the younger event to have produced the overprinting of the age profile.

2131370: foliated granite, drill hole KD0005

Sample	**2131370**		
Collector:	A. Reid		
Location GDA2020:	491100.83	6750371.5	Zone 53
Location Lat-Long:	-29.3758253	134.908299	
250K map sheet:	SH5306 COOBER PEDY		
100K map sheet:	5839 Coober Pedy		
Location:	Drill hole KD0005, 130.5-131.9m		
Mineral analysed:	**biotite**		
Date analysed:	22/Nov/2020		
Interpreted age:	1506.5 ± 8.6 Ma		
Age type:	Upper age limit		
Age interpretation:	Cooling age		
Interpreted age:	1430.7 ± 4.1 Ma		
Age type:	Intermediate age limit		
Age interpretation:	Cooling age		
Mineral analysed:	**K-feldspar**		
Date analysed:	24/Nov/2020		
Interpreted age:	1355 ± 5.6 Ma		
Age type:	Upper age limit		
Age interpretation:	Cooling age		
Interpreted age:	1206.2 ± 7.7 Ma		
Age type:	Lower age limit		
Age interpretation:	Cooling age		

BACKGROUND

The sample from drill hole KDD005 is an example of the regional host rock in the vicinity of the Cairn Hill mine and will enable characterisation of the thermal history of the region (Fig. 13). Hall et al. (2018) obtained a ^{207}Pb corrected weighted mean ^{206}Pb/^{238}U age of 1429 ± 29 Ma (MSWD of 1.15) from apatite from sample 2131371 in this drill hole.

Sample 2131370 compliments two samples of biotite analysed by Fraser et al. (2012), located in the vicinity of the Cairn Hill mine. These yielded ages of 1490 ± 8 Ma (sample 2007371062, Biotite gneiss CD93 2 175.7–176.0 m) and 1444 ± 5 Ma (sample 2007371063, Granitic gneiss, DD86EN33 85.1–85.3 m). In addition, there are also four samples of biotite analysed by Forbes et al. (2012) from elsewhere in the Mt Woods region. These ages are older than the biotite dated by Fraser et al. (2012). This suggests that movement along some of the major shear zones in the region, could be responsible for the younger ages for the biotite in the vicinity of Cairn Hill.

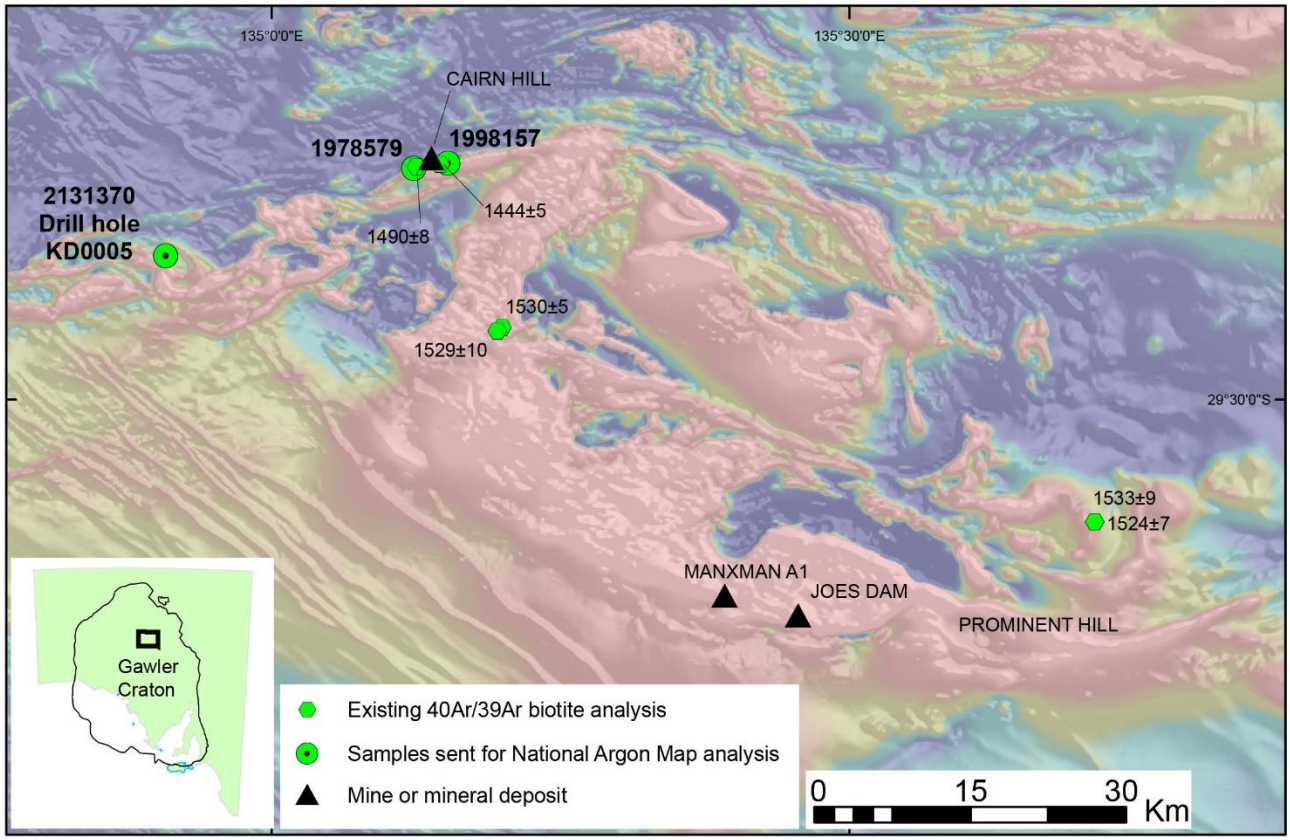

Figure 13. Location map of samples in the vicinity of Cairn Hill Mine. Previous biotite ages are from Fraser et al. (2012) and Forbes et al. (2012).

Sample 2131370 is a biotite-bearing foliated granite (Fig. 14). The sample is from the upper portion of drill hole KDD005, located to the west of Cairn Hill (Garsed et al., 2006). The drill hole intersected dark grey to black, and pink mafic and felsic gneisses in the upper part of the hole, with the lower unit (from about 250 m) dominated by pale grey quartz rich garnet gneiss. From around 230–252 m is a dark grey to green pyroxene-amphibole alteration which is texturally late. There is minor sulphide mineralisation present in this hole.

Figure 14. Photograph of sample 2131370.

PETROGRAPHY

Sample 2131370 is a foliated medium-grained granite (Fig. 15). Quartz occurs as recrystallised aggregates, sometimes ribbons, with minor grain boundary migration and subgrain development. K-feldspar is present and is weakly altered by white mica. Some of the K-feldspar grains are relatively coarse and contain perthitic exsolution as well as recrystallised fringes, suggesting new growth and recrystallisation during deformation of the granite. Plagioclase is extensively altered by white mica. The biotite is brown and occurs as coarse laths that largely define the foliation, and in such examples lies parallel to elongate quartz ribbons and wraps the larger K-feldspar porphyroblasts.

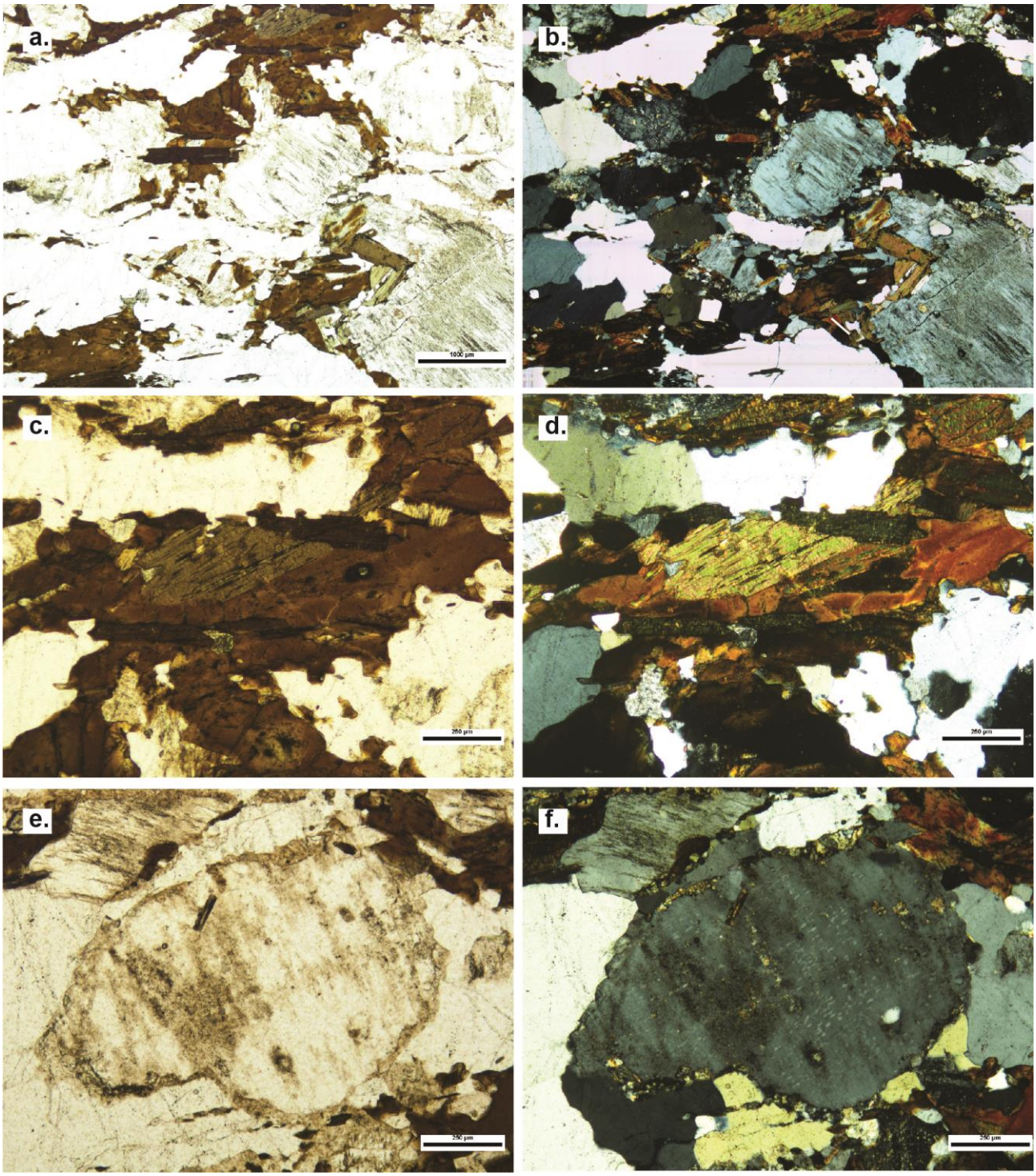

Figure 15. Thin section photomicrograph of sample 2131370, drill hole KDD005. (a) Transmitted plain light. **(b)** Cross polars. **(c)** Detail of biotite in transmitted light. **(d)** Detail of biotite in cross polars. **(e)** Example of coarse K-feldspar grain surrounded by quartz and having a fringe of recrystallised K-feldspar, transmitted plain light. **(f)** Cross polars.

RESULTS

Biotite

The $^{40}Ar/^{39}Ar$ age spectrum for biotite steps upwards from a minimum of c. 210 Ma to an age of 1430.7 ± 4.1 Ma (steps 11, 12, 13, 14; Fig. 16a). The maximum age of the spectrum is step 16 at 1506.5 ± 8.6 Ma. The spectrum then steps downwards through the c. 1430 Ma age at step 16 (included in the age calculation) before decreasing towards the final heating steps at around c. 1300 Ma. There is some scatter in the isotope correlation diagram, however, these scattered points are mostly derived from the early heating steps, and the majority form a cluster (Fig. 16b). The $^{40}Ar^*$ diagram shows that most of the ^{40}Ar is radiogenic, except the early heating steps (Fig. 16c). The Ca/K and Cl/k ratio are relatively consistent with the exception of a spike in Ca/K in the first ~10% gas release (Fig. 16d, e).

K-feldspar

The $^{40}Ar/^{39}Ar$ age spectrum for the K-feldspar from this sample shows two components: the initial steps to around 10% gas released and the remainder of the spectrum (Fig. 17a).

The first 10% gas released has elevated ages in the isothermal heating steps, many of which are geologically unreasonable and a result of excess ^{40}Ar. The correlation between these steps and the elevated $^{36}Ar/^{40}Ar$, low $^{40}Ar^*$ percentage and elevated Ca/K and Cl/K ratios (Fig. 17b, c, d, e) supports the notion that this portion of the age spectrum is from a different gas composition to the remainder of the spectrum. Nevertheless, we note that the maximum age of this first 10% of gas release, at c. 1355 Ma is only slightly younger than the maximum age obtained from the remainder of the age spectrum.

The second portion of the age spectrum is a stepwise rise from a minimum of 1206.2 ± 7.7. Ma to a maximum of 1355 ± 5.6 Ma, defined by an average of the final three steps in the step heating experiment (Fig. 17a). Ca/K and Cl/K across most of the age spectrum is relatively constant, although a slight rise in these values occurs in the final heating steps (Fig. 17d, e).

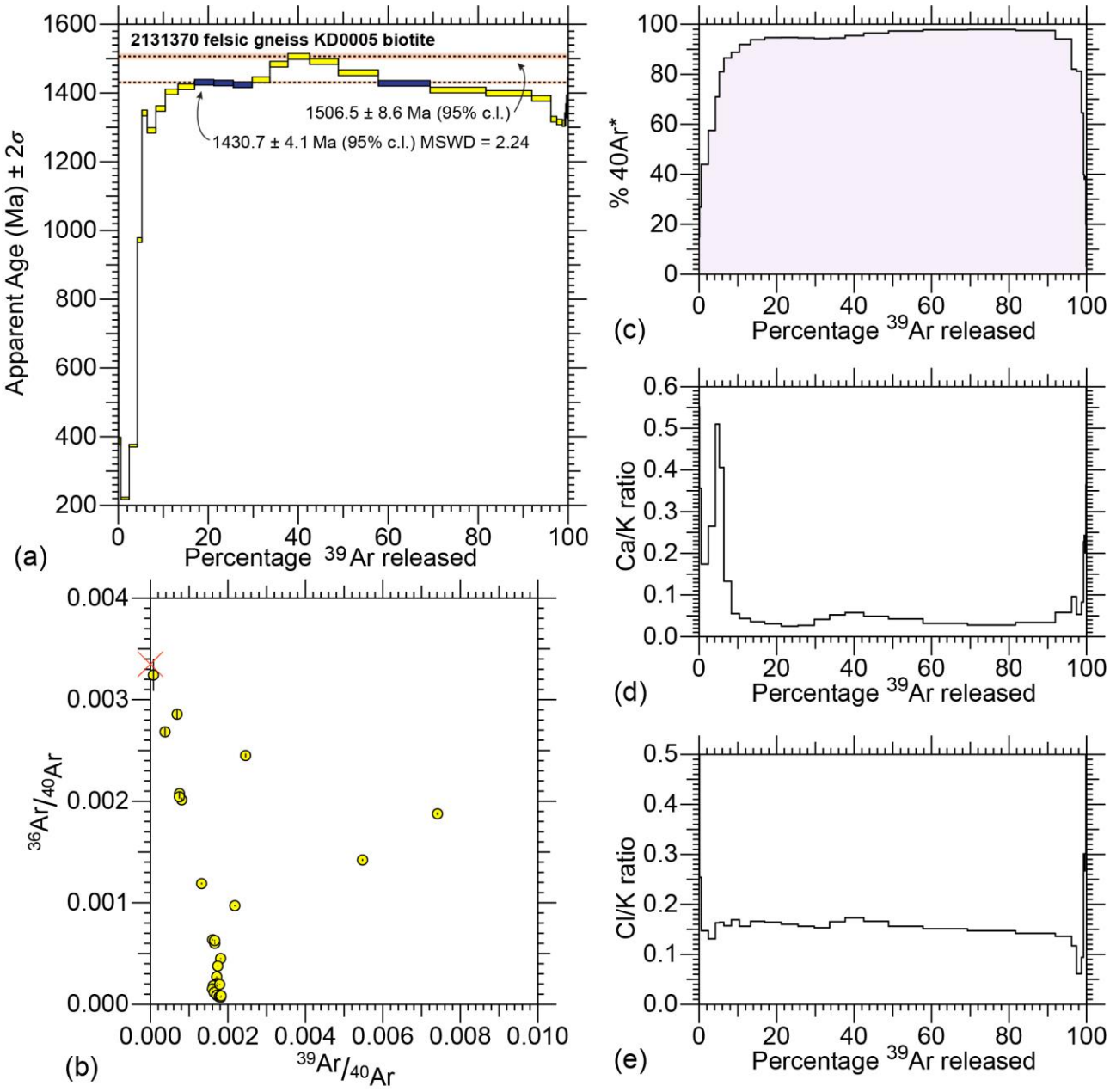

ANU CAN #36, Name: 2131370, Foil: A03, Mineral: Biotite, Mass: 5.1mg, Steps: 30
Australia; SA; near Cairn Hill; Gneiss; Grain Size: 420-250µm
Age 1506 ± 8.5 Ma (95% c.l) Selected step(s): 16
Age 1431 ± 4.1 Ma (95% c.l) Selected step(s): 11 12 13 14
Pearson's chi statistic 1.50 with 95% confidence range f=3 [0.06 - 1.57].

Figure 16. Analytical results for biotite of sample 2131370 (a) age spectrum, (b) isotope correlation diagram, (c) percentage radiogenic ^{40}Ar ($^{40}Ar^*$), (d) Ca/K ratio, and (e) Cl/K ratio.

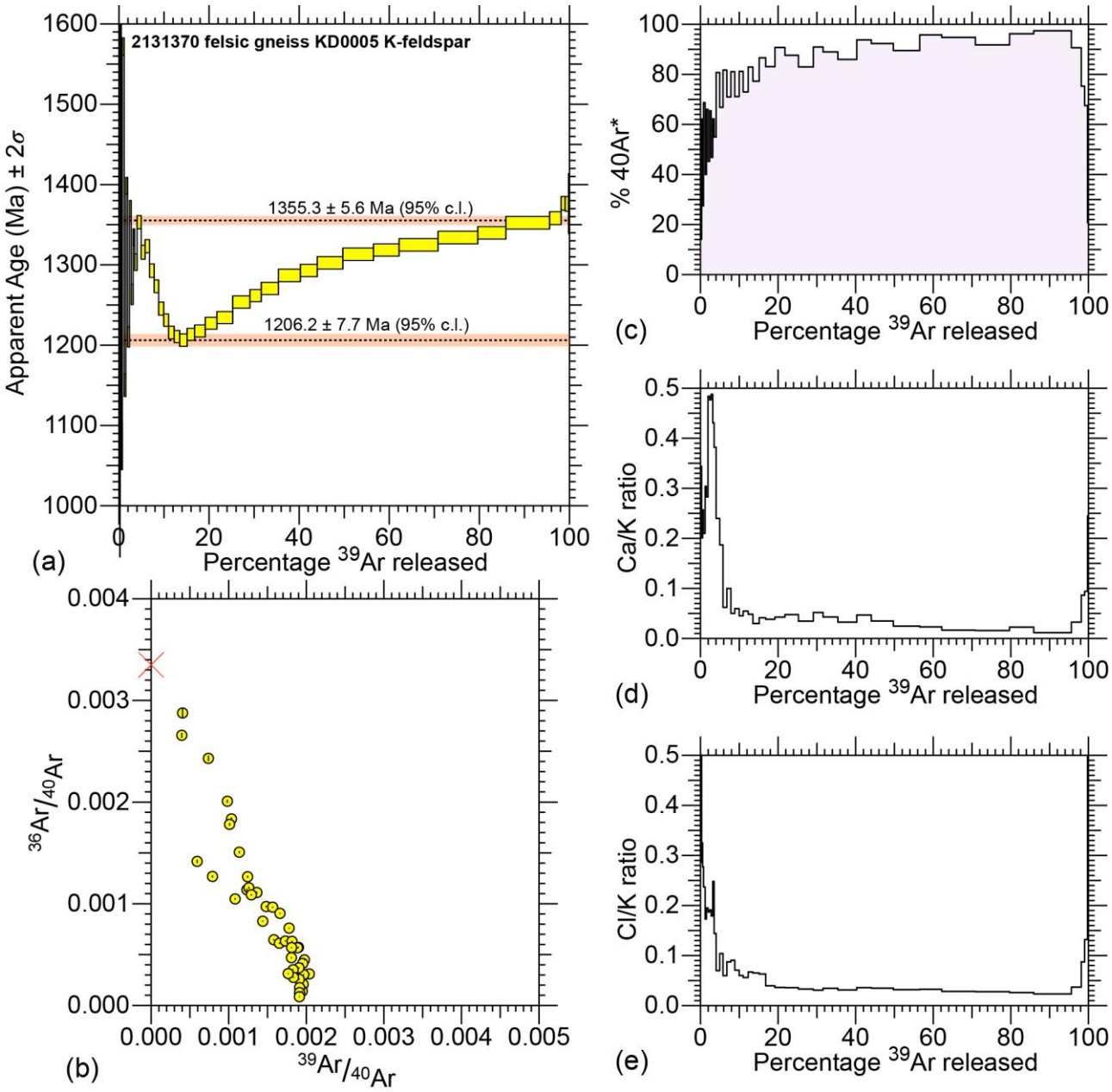

ANU CAN #36, Name: 2131370, Foil: A04, Mineral: K-Feldspar Fine, Mass: 3.2mg, Steps: 42

Australia; SA; near Cairn Hill; Gneiss; Grain Size: 420-250µm

Age 1355.3 ± 5.6 Ma (95% c.l) Selected step(s): 38 39

Age 1206.2 ± 7.7 Ma (95% c.l) Selected step(s): 22

Figure 17. Analytical results for K-feldspar of sample 2131370 (a) age spectrum, (b) isotope correlation diagram, (c) percentage radiogenic ^{40}Ar ($^{40}Ar^*$), (d) Ca/K ratio, and (e) Cl/K ratio.

GEOCHRONOLOGICAL INTERPRETATION

Biotite from this sample suggests initial cooling recorded in the upper age limit of c. 1506 Ma, and that a possible thermal event overprinted the biotite at around c. 1430.7 Ma. The older age of this age spectrum is similar to, but slightly younger than some of the ages recorded elsewhere in the Mt Woods region, c. 1540 – 1530 Ma (Forbes et al., 2012). The c. 1430.7 Ma minimum age is similar to the timing of a widespread thermal event across much of the northern Gawler Craton between c. 1460 – 1415 Ma (Morrissey et al., 2019; Reid and Forster, 2021).

The K-feldspar from this sample records maximum age of c. 1355.3 Ma and minimum age of 1206.2 Ma. The continuous age spectrum between the upper and lower limit suggests that a thermal and or metasomatic event overprinted the K-feldspar at c. 1206.2 Ma. Recrystallisation of the K-feldspar may also have occurred, with some sub-grains evident in the thin section. Further work on the closure temperature profiles for the K-feldspar in this sample may assist in defining the temperature evolution of this event.

SUMMARY OF RESULTS AND SUGGESTIONS FOR FURTHER WORK

The results from the Olympic Dam region suggest that processes in the Mesoproterozoic and also Neoproterozoic-Cambrian have affected the rocks that have been sampled in this National Argon Map project. The recovery of such young signatures in the heavily altered rocks supports the notion that the region of the hematite IOCG deposits in the Gawler Craton has been subject to multiple overprinting thermal and or metasomatic events. The coarse white mica in drill hole ASD 1 must have formed sometime before c. 956 Ma, however, the presence of a c. 499 Ma minimum age suggests that effects of the c. 514 – 490 Ma Delamerian Orogeny are also recorded in these rocks.

The Blanche 1 K-feldspar sample is a stunning example of the multitude of ages that can be recorded within K-feldspar. Previous work has suggested that K-feldspar can contain extremely retentive domains, able to record argon ages that come close to the magmatic age in relatively simple rock systems (Forster and Lister, 2010; Forster et al., 2015). While the upper age limit from the K-feldspar of sample 2111462 is approximately 90 million years younger than the zircon U-Pb magmatic age of the same rock, it is very old in comparison to the remainder of the ages in the age spectrum. Further work on the degree of resetting of K-feldspar in the rock, along with work on the diffusion data derived from Arrhenius information will likely yield insights into the metasomatic growth events recorded in this K-feldspar sample. The fact that the sample has both Musgravian and Neoproterozoic ages suggests hydrothermal processes caused by large-scale geological processes that have affected the South Australian crust are recorded in the Olympic Dam region. This is supported by limited evidence for some degree of fluid overprinting recorded within Olympic Dam deposit itself (e.g. McInnes et al., 2008).

The results from the samples at Cairn Hill also suggest significant Mesoproterozoic and Neoproterozoic thermal and/or metasomatic overprinting has affected the region. Within the Cairn Hill deposit itself, further work is required to investigate a range of geochronometers and document various alteration phases. The samples from drill hole KDD005 further extend the footprint of c. 1465 – 1410 Ma thermal processes recorded elsewhere in the northern Gawler Craton (Reid and Forster, 2021). The K-feldspar data from KDD005 also suggest Musgravian-age thermal or microstructural processes have affected this region, further hinting at the extent of this tectonic system that has affected the South Australian crust.

ACKNOWLEDGEMENTS

AuScope provided the funding to undertake $^{40}Ar/^{39}Ar$ analyses reported here as part of the National Argon Map project. The Geological Survey of South Australia provided funding for thin section and mineral separation processing. Dillon Brown provided a helpful review of this report. Marnie Forster acknowledges support from MinEx Cooperative Research Centre and this document is MinEx CRC document xxxx/xxxx.

REFERENCES

Beyer, S.R., Kyser, K., Polito, P.A., Fraser, G.L., 2018. Mesoproterozoic rift sedimentation, fluid events and uranium prospectivity in the Cariewerloo Basin, Gawler Craton, South Australia. *Australian Journal of Earth Sciences*, 1-18.

Cherry, A.R., Ehrig, K., Kamenetsky, V.S., McPhie, J., Crowley, J.L., Kamenetsky, M.B., 2018. Precise geochronological constraints on the origin, setting and incorporation of ca. 1.59 Ga surficial facies into the Olympic Dam Breccia Complex, South Australia. *Precambrian Research* 315, 162-178.

Courtney-Davies, L., Ciobanu, C.L., Tapster, S.R., Cook, N.J., Ehrig, K., Crowley, J.L., Verdugo-Ihl, M.R., Wade, B.P., Condon, D.J., 2020. Opening the magmatic-hydrothermal window: high-precision U-Pb geochronology of the Mesoproterozoic Olympic Dam Cu-Au-U-Ag deposit, South Australia. *Economic Geology*.

Ehrig, K., McPhie, J., Kamenetsky, V., 2012. Geology and mineralogical zonation of the Olympic Dam iron oxide Cu-U-Au-Ag deposit, South Australia, in: Hedenquist, J.W., Harris, M., Camus, F. (Eds.), *Geology and genesis of major copper deposits and districts of the world: A tribute to Richard H. Sillitoe*. Society of Economic Geologists Special Publication 16, pp. 237-267.

Forbes, C.J., Giles, D., Jourdan, F., Sato, K., Omori, S., Bunch, M., 2012. Cooling and exhumation history of the northeastern Gawler Craton, South Australia. *Precambrian Research* 200–203, 209-238.

Forster, M.A., Armstrong, R., Kohn, B., Lister, G.S., Cottam, M.A., Suggate, S., 2015. Highly retentive core domains in K-feldspar and their implications for 40Ar/39Ar thermochronology illustrated by determining the cooling curve for the Capoas Granite, Palawan, The Philippines. *Australian Journal of Earth Sciences* 62, 883-902.

Forster, M.A., Lister, G.S., 2004. The interpretation of 40Ar/39Ar apparent age spectra produced by mixing: application of the method of asymptotes and limits. *Journal of Structural Geology* 26, 287-305.

Forster, M.A., Lister, G.S., 2010. Argon enters the retentive zone: reassessment of diffusion parameters for K-feldspar in the South Cyclades Shear Zone, Ios, Greece, in: Spalla, M.I., Marotta, A.M., Gosso, G. (Eds.), *Advances in Interpretation of Geological Processes: Refinement of Multi-scale Data and Integration in Numerical Modelling*. Geological Society of London.

Forster, M.A., Lister, G.S., Spalla, M.I., Marotta, A.M., Gosso, G., 2010. *Argon enters the retentive zone: reassessment of diffusion parameters for K-feldspar in the South Cyclades Shear Zone, Ios, Greece, Advances in Interpretation of Geological Processes: Refinement of Multi-scale Data and Integration in Numerical Modelling*. Geological Society of London, p. 0.

Fraser, G., Reid, A., Stern, R., 2012. Timing of deformation and exhumation across the Karari Shear Zone, north-western Gawler Craton, South Australia. *Australian Journal of Earth Sciences* 59, 547-570.

Garsed, I.R., Manzi, B., Purvis, A.C., 2006. Unlocking South Australia's Mineral and Energy Potential - A Plan for Accelerating Exploration. Theme 2 (drilling partnerships with PIRSA and industry) : Year 2 partnership no. DPY2-35, Mount Woods Inlier, Kangaroo Dam platinoid metals mineral prospect. Project final report. South Australia. Department of Primary Industries and Resources. Open file Envelope, 11161. https://sarigbasis.pir.sa.gov.au/WebtopEw/ws/samref/sarig1/image/DDD/ENV11161.pdf

Hall, J.W., Glorie, S., Reid, A.J., Collins, A.S., Jourdan, F., Danišík, M., Evans, N., 2018. Thermal history of the northern Olympic Domain, Gawler Craton; correlations between thermochronometric data and mineralising systems. *Gondwana Research* 56, 90-104.

Jagodzinski, E.A., Crowley, J.L., Reid, A.J., Wade, C.E., Bockmann, M.J., 2021. *High-precision CA-TIMS dating of the Hiltaba Suite, Gawler Craton*. Report Book, 2021/00002. Department for Energy and Mining. Government of South Australia. https://sarigbasis.pir.sa.gov.au/WebtopEw/ws/samref/sarig1/image/DDD/RB202100002.pdf

Jagodzinski, E.A., Reid, A.J., 2015. *PACE Geochronology: Results of collaborative geochronology projects, 2013-2015*. Report Book, 2015/00003. Department of the Premier and Cabinet. Government of South Australia. https://sarigbasis.pir.sa.gov.au/WebtopEw/ws/samref/sarig1/image/DDD/RB201500003.pdf

Lovera, O.M., Grove, M., Mark Harrison, T., Mahon, K.I., 1997. Systematic analysis of K-feldspar 40Ar39Ar step heating results: I. Significance of activation energy determinations. *Geochimica et Cosmochimica Acta* 61, 3171-3192.

McInnes, B.I.A., Keays, R.R., Lambert, D.D., Hellstrom, J., Allwood, J.S., 2008. Re-Os geochronology and isotope systematics of the Tanami, Tennant Creek and Olympic Dam Cu-Au deposits. *Australian Journal of Earth Sciences* 55, 967-981.

Meyer, G., 2006. Blanche 001 Geothermal Exploration Hole Completion Report. 08098/000.

Morrissey, L.J., Barovich, K.M., Hand, M., Howard, K.E., Payne, J.L., 2019. Magmatism and metamorphism at ca. 1.45 Ga in the northern Gawler Craton: The Australian record of rifting within Nuna (Columbia). *Geoscience Frontiers* 10, 175-194.

Muston, J., Forster, M., Vasegh, D., Alderton, C., Crispin, S., Lister, G., 2021. Direct dating of overprinting fluid systems in the Martabe epithermal gold deposit using highly retentive alunite. *Geochronology Discuss*. 2021, 1-31.

Pownall, J.M., Forster, M.A., Hall, R., Watkinson, I.M., 2017. Tectonometamorphic evolution of Seram and Ambon, eastern Indonesia: Insights from 40Ar/39Ar geochronology. *Gondwana Research* 44, 35-53.

Reid, A., 2019. The Olympic Cu-Au Province, Gawler Craton: A Review of the Lithospheric Architecture, Geodynamic Setting, Alteration Systems, Cover Successions and Prospectivity. *Minerals* 9, 371.

Reid, A., Forster, M., 2021. Mesoproterozoic thermal evolution of the northern Gawler Craton from 40Ar/39Ar geochronology. *Precambrian Research* 358, 106180.

Reid, A.J., Jourdan, F., Jagodzinski, E.A., 2017. Mesoproterozoic fluid events affecting Archean crust in the northern Olympic Cu–Au Province, Gawler Craton: insights from 40Ar/39Ar thermochronology. *Australian Journal of Earth Sciences* 64, 103-119.

Renne, P.R., Balco, G., Ludwig, K.R., Mundil, R., Min, K., 2011. Response to the comment by W.H. Schwarz et al. on "Joint determination of 40K decay constants and 40Ar∗/40K for the Fish Canyon sanidine standard, and improved accuracy for 40Ar/39Ar geochronology" by P.R. Renne et al. (2010). *Geochimica et Cosmochimica Acta* 75, 5097-5100.

Skirrow, R.G., 2010. 'Hematite-group' IOCG±U ore systems: Tectonic settings, hydrothermal characteristics, and Cu-Au and U mineralizing processes, in: Corriveau, L., Mumin, H. (Eds.), *Exploring for Iron Oxide Copper-Gold Deposits: Canada and Global Analogues. Shortcourse Notes, GAC-MAC-SEG-SGA 2008, Quebec City, 29-30th May 2008*. Geological Association of Canada, pp. 39-58.

Skirrow, R.G., Bastrakov, E.N., Barovich, K., Fraser, G.L., Creaser, R.A., Fanning, C.M., Raymond, O.L., Davidson, G.J., 2007. Timing of iron oxide Cu-Au-(U) hydrothermal activity and Nd isotope constraints on metal sources in the Gawler Craton, South Australia. *Economic Geology* 102, 1441-1470.

Spell, T.L., McDougall, I., 2003. Characterization and calibration of 40Ar/39Ar dating standards. *Chemical Geology* 198, 189-211.